Available online at www.sciencedirect.com
ScienceDirect
Biochimica et Biophysica Acta 1768 (2007) 366–374
Biochimica et Biophysica Acta
BBA
www.elsevier.com/locate/bbamem

The pH-dependent distribution of the photosensitizer chlorin e6 among plasma proteins and membranes: A physico-chemical approach

Halina Mojzisova, Stephanie Bonneau, Christine Vever-Bizet, Daniel Brault *

Laboratoire de Biophysique Moléculaire Cellulaire and Tissulaire (BIOMOCETI) CNRS UMR 7033, Université Pierre and Marie Curie, Genopole Campus 1, 5 rue Henri Desbruères, 91030 EVRY cedex, France

Received 18 July 2006; received in revised form 22 September 2006; accepted 18 October 2006
Available online 25 October 2006

Abstract

Decrease in interstitial pH of the tumor stroma and over-expression of low density lipoprotein (LDL) receptors by several types of neoplastic cells have been suggested to be important determinants of selective retention of photosensitizers by proliferative tissues. The interactions of chlorin e6 (Ce6), a photosensitizer bearing three carboxylic groups, with plasma proteins and DOPC unilamellar vesicles are investigated by fluorescence spectroscopy. The binding constant to liposomes, with reference to the DOPC concentration, is 6×10^3 M^{-1} at pH 7.4. Binding of Ce6 to LDL involves about ten high affinity sites close to the apoprotein and some solubilization in the lipid compartment. The overall association constant is 5.7×10^7 M^{-1} at pH 7.4. Human serum albumin (HSA) is the major carrier (association constant 1.8×10^8 M^{-1} at pH 7.4). Whereas the affinity of Ce6 for LDL and liposomes increases at lower pH, it decreases for albumin. Between pH 7.4 and 6.5, the relative affinities of Ce6 for LDL versus HSA, and for membranes versus HSA, are multiplied by 4.6 and 3.5, respectively. These effects are likely driven by the ionization equilibria of the photosensitizer carboxylic chains. Then, the cellular uptake of chlorin e6 may be facilitated by its pH-mediated redistribution within the tumor stroma.

Keywords: Photosensitizer; pH; Albumin; Lipoprotein; Model membranes

1. Introduction

The therapeutic use of photosensitizing drugs is based on light-induced generation of reactive species that damage surrounding biological structures [1]. The selective accumulation of photosensitizers in proliferating tissues and the possibility to define the limits of the irradiated zone are two main factors insuring the specificity of photodynamic action [2]. The space diffusion of the reactive species, namely oxyradicals and singlet oxygen, is limited by their extremely short life time [3]. Thus the extent of the photoinduced damage is restricted to the structures labeled by the photosensitizer. Consequently, the uptake and/or retention of photosensitizers by targeted cells or tissues are crucial determinants of their efficiency. Several explanations have been proposed to clarify the selective uptake of porphyrin-type photosensitizers by neoplastic tissues. Firstly, extracellular accumulation of lactic acid results in the acidification of tumor interstitial matrix [4,5]. Consistent data obtained on cultured cells [6,7], animals [8] and membrane models [9] present strong evidence for a major role of the pH gradient thus created in the selective tumoral uptake of photosensitizers bearing carboxylic chains.

Another important determinant of the cellular incorporation of photosensitizers is their binding to low density lipoproteins (LDL). This association influences both the overall cellular uptake and the internalization pathway of the drug. The role of lipoproteins as blood carriers of photosensitizers has been proposed by several authors [10–12]. LDL are considered as a targeting and delivery system of lipophilic or amphiphilic photosensitizers [13]. Moreover, increased cholesterol requirements of proliferating tissues result in the over-expression of LDL receptors on the cell surface [14,15]. Thus, the cellular incorporation of lipoprotein bound photosensitizers via LDL-specific endocytosis has been suggested to be one of the main mechanisms of their preferential accumulation by tumors. Low-

* Corresponding author. Fax: + 33 1 69 87 43 60.
E-mail address: dbrault@ccr.jussieu.fr (D. Brault).

0005-2736/$ - see front matter © 2006 Elsevier B.V. All rights reserved.
doi:10.1016/j.bbamem.2006.10.009

density lipoproteins are nearly spherical, highly plastic particles with diameters of between 210 and 250 Å. The LDL lipid core containing cholesteryl esters and triglycerides is surrounded by a monolayer of cholesterol and phospholipids. The large apoprotein B100 (500 kDa), associated to the phospholipid envelope, contributes to the overall structure of the particle and ensures its recognition by cellular receptors [16]. The number of photosensitizers bound to LDL and their localization within these particles are important determinants of this transportation mode.

In addition, the bioavailability of photosensitizers is governed by the competitive binding to albumin, the major protein in plasma [17]. The distribution of certain photosensitizers with various degrees of lipophilicity and numbers of charges among plasma proteins has been studied by means of ultracentrifugation [18–21]. A general finding was that the fraction of the dyes bound to LDL increased, and the fraction bound to HSA decreased with decreasing polarity of the dyes. However, the relative binding to these proteins was also dependent on the position of charges around the macrocycle [18]. It must be noted that the permeability of neovessels may allow leakage of albumin-bound photosensitizers into the tumor stroma, which would also lead to some selective retention [22].

In this study, we consider chlorin e6 (Ce6) that bears three carboxylic groups (see Fig. 1). This molecule was chosen as it enabled to the verification of the effect of the number of carboxylic groups when compared to dicarboxylic porphyrins. It is also relevant to therapy as a second-generation photosensitizer [23]. Quantitative data on the interactions of Ce6 with various potential serum carriers, as well as with cell-mimicking membrane systems, are derived in this paper. The effect of pH is particularly emphasized.

2. Material and Methods

2.1. Chemicals

Chlorin e6 (Fig. 1) was purchased from Porphyrin Products, Logan (UT, USA). A stock solution (1 mM) was prepared in 20 mM $Na_2H\ PO_4$. The experimental Ce6 solutions were diluted in phosphate buffer saline, PBS (20 mM KH_2PO_4/Na_2HPO_4, 150 mM NaCl, pH indicated for each experiment) and handled in the dark.

Human serum albumin (HSA) was purchased from Sigma (St. Louis, MO, USA). Experimental solutions were prepared in PBS at the desired pH and were used immediately.

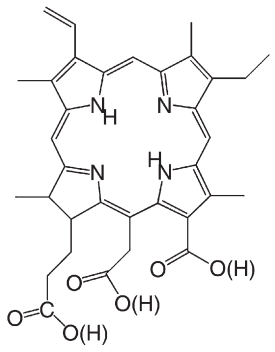

Fig. 1. Structure of chlorin e6.

Human low-density lipoproteins (LDL) were purchased from Calbiochem (San Diego, CA, USA). They were conditioned at a concentration of 9.52 mg/ml (protein content) in 150 mM NaCl pH 7.4 aqueous solution with 0.01% EDTA.

Dioleyol-*sn*-phosphatidylcholine (DOPC) was purchased from Avanti Polar Lipids (Alabaster, AL, USA). Chloroform (Merck, Darmstadt, Germany) was of spectroscopic grade quality. Triton X-100 was purchased from Sigma (St. Louis, MO, USA).

2.2. Liposome preparation

DOPC was dissolved in chloroform and the solution was taken to dryness. The lipid film obtained was rehydrated in PBS and vortexed for several minutes. The liposome suspension was extruded 10 times through a stack of two polycarbonate membrane filters (Poretics, Livermore, CA, USA) with a pore size of 50 nm using an extruder device (Lipex, Biomembranes, Vancouver, Canada).

2.3. Fluorescence measurements

Fluorescence measurements were performed with an Aminco Bowman Series 2 spectrofluorimeter. The samples were contained in a 1 cm quartz cell and were stirred during the acquisition.

2.3.1. Partition experiments: Incorporation of Ce6 in DOPC vesicles

For experiments at equilibrium, the DOPC liposome solutions were prepared at different concentrations. 10 μL of 10 μM Ce6 solution were added to 2 ml of vesicle preparation and the fluorescence spectra were recorded. In order to correct the spectra for small differences in Ce6 concentration arising from experimental inaccuracy, 20 μL of Triton-X100 were added after measurement leading to disruption of vesicles and solubilization of all Ce6 in the Triton micelles. The spectra were normalized accordingly.

The global binding constant, K_B, was derived from changes in the fluorescence signal at a wavelength corresponding to the maximum of fluorescence emission of Ce6 incorporated into the membrane. We used the previously derived relationship [24]:

$$F = F_0 + \frac{(F\infty - F_0) \times K_B \times [\mathrm{DOPC}]}{1 + K_B \times [\mathrm{DOPC}]} \quad (1)$$

where F_0, F_∞ and F are the fluorescence intensities corresponding to zero, total and intermediate incorporation of chlorin into vesicles, respectively. DOPC being in large excess, the saturation of the bilayer is far to be reached and it can be assumed that Ce6 binding does not affect the properties of the model membrane. Then, regardless of the number of Ce6 molecules incorporated into a vesicle, [DOPC] was assumed to be equivalent to the total DOPC concentration added.

2.3.2. Binding to HSA and LDL

Contrary to former partition experiments, the interactions of Ce6 with HSA and LDL involved a limited number of sites. Moreover, due to the high affinity of chlorin to HSA and LDL, the concentration of Ce6 and that of the macromolecules were of the same order of magnitude in our experimental conditions. Consequently, the concentration of free sites on HSA or LDL was calculated by subtracting the amount of bound chlorin to the total number of binding sites per molecule. For this purpose, the concentrations of free and bound Ce6 were calculated by a spectral decomposition program running with the MatLab® (MathWorks, Natick, MA) software according to the equation:

$$(\mathrm{SP}) = \begin{pmatrix} Comp1 \\ Comp2 \end{pmatrix} \times (f_{\mathrm{PBS}}, f_B) \quad (2)$$

where SP is the experimental spectrum, Comp1 and Comp2 are the spectra of Ce6 in PBS and bound to the macromolecule, respectively. Comp2 was obtained using an excess of the macromolecule to insure total binding. The relative concentrations of free and bound chlorin are given by the factors f_{PBS} and f_B.

The equilibrium of Ce6 binding to the plasma proteins can be written as:

$$[\mathrm{Chl}]_F + [\mathrm{P}]_F \underset{}{\overset{K_B}{\rightleftharpoons}} [\mathrm{Chl}]_B$$

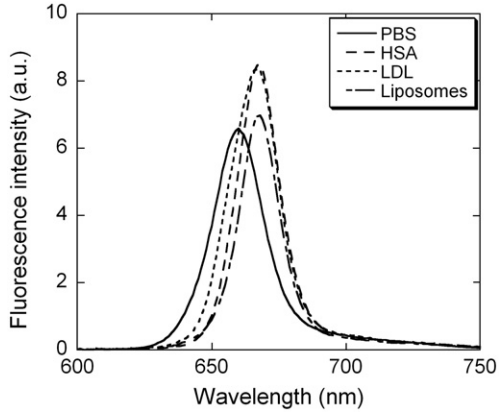

Fig. 2. Fluorescence emission spectra of Ce6 (5×10^{-8} M) in phosphate buffer (pH=7.4) and in presence of LDL (4×10^{-7} M), HSA (5×10^{-6} M) and DOPC (1.9×10^{-3} M), λ_{exc}=410 nm. The shoulder on the blue side of the spectrum in presence of LDL corresponds to the unbound fraction of Ce6.

where $[Chl]_F$ and $[Chl]_B$ are free and bound Ce6 concentrations, respectively. The overall binding constant is defined as:

$$K_B = \frac{[Chl]_B}{[Chl]_F \times [P]_F} \tag{3}$$

Assuming that n_P is the number of binding sites per protein, $n_P\, x[P]_F$ is the averaged concentration of free protein sites. The total protein concentration being $[P]_{tot}$, it follows:

$$[P]_F = \left([P]_{tot} - \frac{[Chl]_B}{n_P}\right) \tag{4}$$

Combining Eqs. (3) and (4) leads to:

$$[Chl]_B = \frac{[Chl]_{tot} \times K_B \times \left([P]_{tot} - \frac{[Chl]_B}{n_P}\right)}{1 \times \left([P]_{tot} - \frac{[Chl]_B}{n_P}\right) \times K_B} \tag{5}$$

2.3.3. Förster's distance determination

According to Förster's theory of resonant energy transfer, the distance at which half of energy emitted by the donor is absorbed by the acceptor, also called the Förster's radius is given by:

$$R_0^6 = 8.8 \times 10^{-25} \times (J \times \kappa^2 \times \Phi_D \times n^{-4})[\mathrm{cm}] \tag{6}$$

where κ is the dipole–dipole orientation factor, n the refractive index of the medium, Φ_D the donor fluorescence quantum yield in absence of acceptor. The spectral overlap between the donor fluorescence and acceptor absorbance spectrum, J, is given by:

$$J = \frac{\int f_D(\lambda) \times \varepsilon_A(\lambda) \times \lambda^4 d\lambda}{\int f_D(\lambda) d\lambda} \tag{7}$$

The relationship between the energy transfer efficiency E and the donor–acceptor distance r is:

$$E = 1 - \frac{F_\infty}{F_0} = \frac{R_0^6}{(R_0^6 + r^6)} \tag{8}$$

where F_∞ and F_0 are the donor fluorescence intensities in presence and absence of the acceptor, respectively.

In the case of LDL–Ce6 interaction, we used the values κ=0.66 for a random orientation, Φ_D=0.11 for the fluorescence quantum yield of tryptophan in hydrophobic environment [25], and n=1.4 for the refractive index of the aqueous buffer.

3. Results

The fluorescence emission spectra of Ce6 in PBS, bound to HSA, LDL and DOPC liposomes are presented in Fig. 2. HSA, LDL or DOPC do not emit any fluorescence in the spectral region between 500 and 750 nm. Ce6 concentration was 5×10^{-8} M. The excitation wavelength was set at 410 nm, which allows the best discrimination between the various environments. The concentrations of HSA and DOPC were high enough to ensure association of all chlorin molecules (see below). In the case of LDL, a minor non-bound fraction of Ce6 is responsible for the shoulder on the blue part of the spectrum. The fluorescence emission maximum of Ce6 is observed at 660 nm in PBS. It is red-shifted to 668 nm upon binding to HSA or DOPC liposomes and to 667 nm when associated to LDL. Moreover, the fluorescence intensity increases. These spectral changes are specific for the transfer of chlorin from an aqueous to a hydrophobic environment [26]. They are sufficient to allow the spectral decomposition required for the calculation of binding constants as reported in Materials and methods.

Fig. 3 shows the chlorin fluorescence emission spectra in PBS at pH 6.5, 7.4 and 8.0. An important decrease of the fluorescence intensity and a small blue shift (3 nm) of the emission band are observed when the pH is decreased.

3.1. Binding of Ce6 to DOPC liposomes

The interaction of Ce6 (5×10^{-8} M) with liposomes was considered as a partition of the photosensitizer between the bulk aqueous medium and the phospholipid bilayer. In the range of concentrations used, the DOPC/Ce6 ratio was at least 500. It was assumed that the binding of one Ce6 molecule does not influence the fixation of others in our experimental conditions, which means that the membrane presents an unlimited number of "binding sites". The fluorescence emission spectra of Ce6 at different DOPC concentrations are shown in Fig. 4a. The excitation wavelength was set at 408 nm, the fluorescence excitation maximum of chlorin bound to liposomes. Fig. 4b shows the changes of the fluorescence intensity at 670 nm, the fluorescence emission maximum of Ce6 incorporated into the

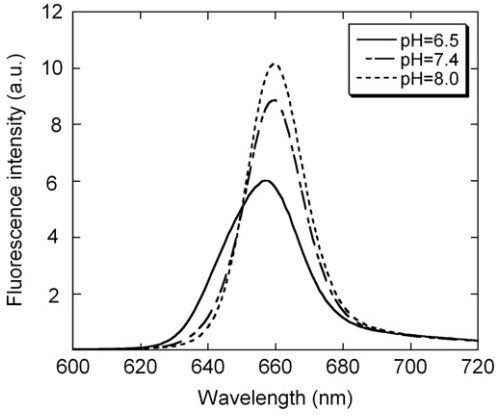

Fig. 3. Fluorescence emission spectra of chlorin e6 (5×10^{-8} M) in PBS buffered at pH 6.5, 7.4 and 8.0, λ_{exc}: 400 nm.

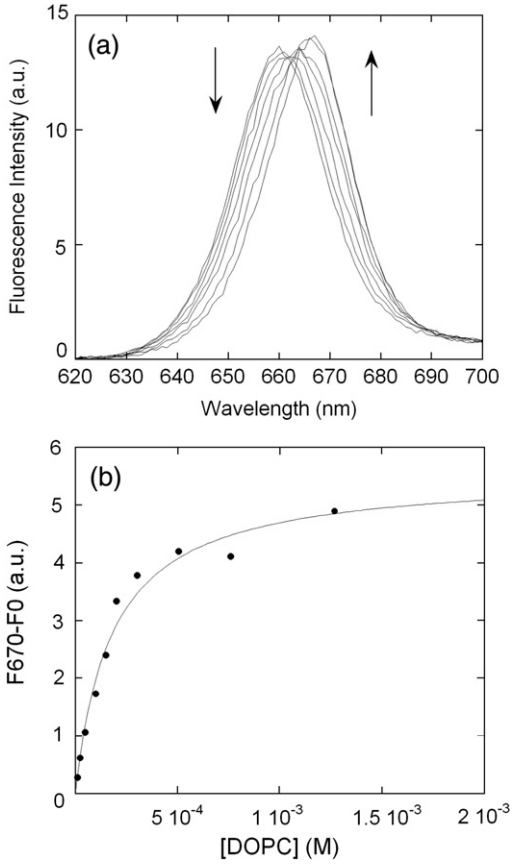

Fig. 4. Evolution of fluorescence emission of Ce6 (5×10^{-8} M) upon incorporation into DOPC liposomes at pH 7.4. The excitation wavelength was set at 408 nm. (a) Fluorescence emission spectra. The DOPC concentration was 0, 0.17, 0.86, 1.73, 2.59, 4.75, and 6.48×10^{-4} M. The arrows indicate changes upon liposome addition. (b) Evolution of the fluorescence intensity at 670 nm. Experimental data are fitted according to Eq. (1) with an association constant K_{DOPC} of 5.9×10^{3} M.

liposomes, upon DOPC concentration increase. The binding constant value was determined by fitting the experimental data to Eq. (1) (Fig. 4b). K_{DOPC} values increase by one order of magnitude in the pH range between 8.0 and 6.5 (Table 1).

3.2. Binding of Ce6 to HSA

Fluorescence emission spectra of Ce6 (5×10^{-9} M) solutions containing increasing amounts of HSA were recorded with an excitation wavelength set at 408 nm, the excitation maximum of Ce6 bound to HSA. Due to the high affinity of the chlorin towards HSA, the equilibrium conditions necessary to determine an equilibrium constant are attained only at very low protein concentrations. As a consequence, the Ce6 and HSA concentrations were of the same order of magnitude in our experimental conditions and it was not possible to assume that free protein binding sites were in excess. Hence, the concentrations of free and bound chlorin ($[Chl]_F$ and $[Chl]_B$) were determined by spectral decomposition according to Eq. (2). The total chlorin concentration, $[Chl]_{tot}$, was a constant in our experimental conditions. The free HSA concentration was calculated by assuming n_{HSA} equal to 1. Fitting data by using Eq. (5) yielded the same affinity constant value, K_{HSA}, independently of the Ce6 concentration. Typical fits are shown in Fig. 5a. Interestingly, binding of Ce6 to HSA was pH-dependent with a binding constant decreasing at lower pH (see Table 1).

Table 1
Ce6 binding constants (M^{-1})

pH	6.5	7.4	8.0
K_{DOPC} *	$(9.1\pm0.6)\times10^{3}$	$(5.9\pm1.1)\times10^{3}$	$(2.3\pm0.4)\times10^{3}$
K_{HSA}	$(0.8\pm0.1)\times10^{8}$	$(1.8\pm0.2)\times10^{8}$	$(3.2\pm0.6)\times10^{8}$
K_{LDL}	(a) $(12.2\pm1.7)\times10^{7}$	(a) $(6.9\pm1.0)\times10^{7}$	
		(b) $(5.7\pm1.0)\times10^{7}$	

Values (a) and (b) for LDL were obtained from data shown in Fig. 5b and Fig. 7, respectively.

* These values should be divided by 0.558 if only the outer hemileaflet of liposomes is populated (see Discussion).

3.3. Binding of Ce6 to LDL

3.3.1. Quenching of the LDL fluorescence by Ce6

Apoprotein B-100 contains 37 tryptophan and 151 tyrosine residues that are responsible for the LDL fluorescence emission at 333 nm. The overlap between the emission spectrum of LDL and absorption spectrum of LDL bound Ce6 (Fig. 6a) indicates that the resonant energy transfer from Trp–Tyr residues to Ce6

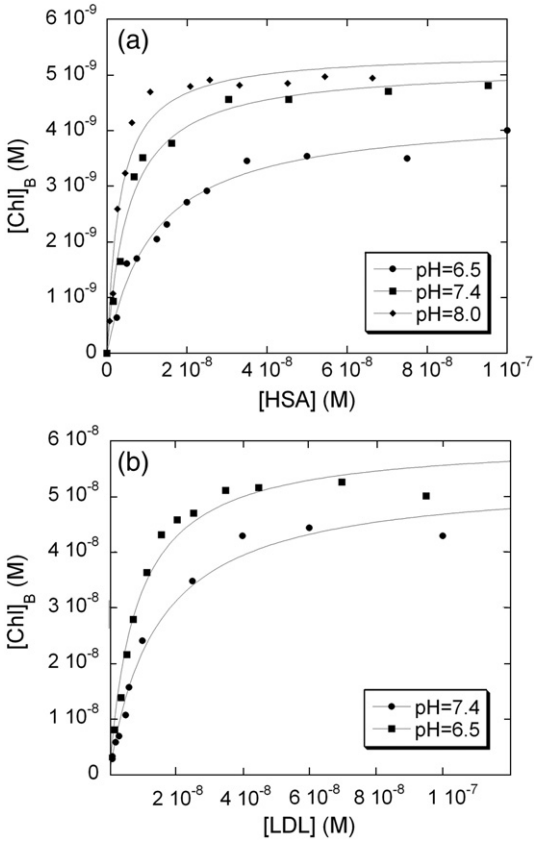

Fig. 5. Binding of Ce6 to HSA (a) and LDL (b) at various pH. Data are fitted according to Eq. (5). The association constants thus obtained are given in Table 1.

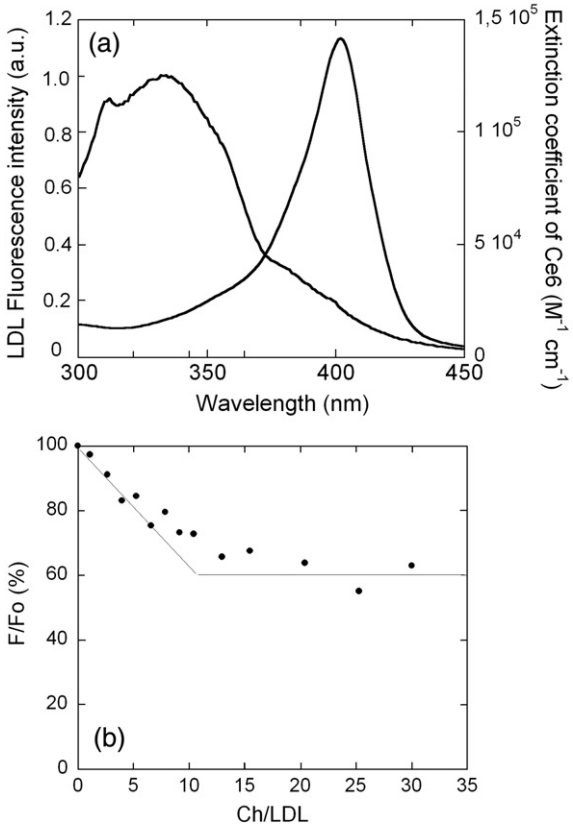

Fig. 6. (a) Fluorescence emission spectrum of LDL (excitation 280 nm, left) and extinction coefficient spectrum of LDL-bound Ce6 (right). (b) Quenching of LDL intrinsic fluorescence upon binding of chlorin e6. [LDL]: 6×10^{-8} M, Ce6/LDL: 0.5–30 (excitation wavelength: 280 nm). The fluorescence intensity of LDL without chlorin is normalized to 100%.

is possible. The spectral overlap, J, was calculated to be 6.28×10^{-14} by using Eq. (7) (see Materials and methods). The Försters's distance for the couple LDL–Ce6 calculated according to Eq. (6) is about 3 nm.

The fluorescence emission of LDL solutions (5×10^{-8} M) with the excitation wavelength set at 280 nm was measured in the presence of increasing amounts of Ce6. The Ce6/LDL concentration ratio ranged from 1 to 25. As shown in Fig. 6b, quenching of the emission fluorescence at 333 nm plateaus out at around 40% upon addition of Ce6. According to Eq. (8), the mean distance between tryptophan residues and Ce6 would be about 3.2 nm. Hence, a significant part of Ce6 molecules binds to sites on the Apo B-100 component or in close proximity. In addition, the intercept between the initial slope of the quenching curve and the plateau indicates that approximately ten chlorin molecules are bound per LDL particle.

3.3.2. Ce6 fluorescence-Scatchard's plot

In order to get more information on a possible repartition of Ce6 molecules between different LDL compartments, we measured the changes of fluorescence emission of Ce6 upon binding to LDL. This study was based on a model previously developed by Bonneau et al. [27] that uses Scatchard's method.

Binding of molecules to m different classes of binding sites can be described by the general relationship [28]:

$$v=\sum_{i=1}^{m}\frac{n_i\times K_{\mathrm{i}}\times[\mathrm{Chl}]_{\mathrm{F}}}{1+K_{\mathrm{i}}\times[\mathrm{Chl}]_{\mathrm{F}}} \tag{9}$$

where v is the number of chlorin molecules bound per LDL, $[\mathrm{Chl}]_{\mathrm{F}}$ is the free chlorin concentration at equilibrium, n_{i} is the number of sites for an homogeneous binding class and K_{i} the corresponding intrinsic binding constant. In keeping with former studies [27,29] and the above results, we considered two binding classes. One involves n_{P} sites with an intrinsic association constant K_{Pi} in the proximity of the apoprotein, and the other, binding to the lipid compartment. The latter process is considered as a solubilization in the lipidic LDL moiety and can be represented by a large number of sites n_{Li} with a relatively small intrinsic binding constant K_{Li}. The overall binding equation

$$\frac{v}{[\mathrm{Chl}]_{\mathrm{F}}}=\frac{n_{\mathrm{P}}\times K_{\mathrm{Pi}}}{1+[\mathrm{Chl}]_{\mathrm{F}}\times K_{\mathrm{Pi}}}+\frac{n_{\mathrm{L}}\times K_{\mathrm{Li}}}{1+[\mathrm{Chl}]_{\mathrm{F}}\times K_{\mathrm{Li}}} \tag{10}$$

can be simplified to

$$\frac{v}{[\mathrm{Chl}]_{\mathrm{F}}}=\frac{n_{\mathrm{P}}\times K_{\mathrm{Pi}}}{1+[\mathrm{Chl}]_{\mathrm{F}}\times K_{\mathrm{Pi}}}+K_{\mathrm{L}} \tag{11}$$

with the assumption $[\mathrm{Chl}]_{\mathrm{F}}\times K_{\mathrm{Li}}\ll 1$ and $K_{\mathrm{L}}=n_{\mathrm{Li}}\times K_{\mathrm{Li}}$.

The fluorescence emission spectra of solutions made with a constant LDL concentration (5×10^{-8} M) and increasing Ce6 concentrations were recorded. The Ce6/LDL concentration ratio ranged between 0.1 and 20. Free and bound Ce6 concentrations were calculated for each spectrum according to the procedure described above. The Scatchard's plot (see Fig. 7) shows a curvature indicating that more than one class of sites is involved. Fitting data to Eq. (11) confirms binding to a class representing about 10 sites with a high intrinsic association constant ($K_{\mathrm{Pi}}=5\times10^{6}$ M^{-1}). Binding to the lipidic part with an overall affinity constant $K_{\mathrm{L}}=7\times10^{6}$ M^{-1} account for the

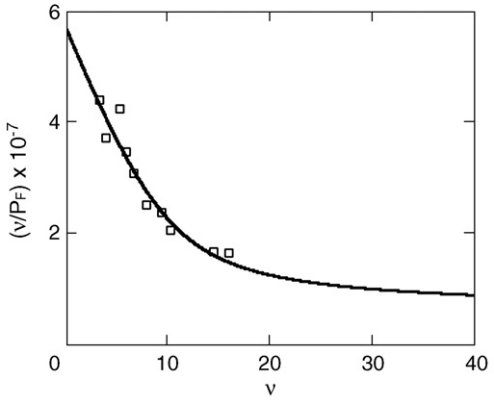

Fig. 7. Scatchard's plot of the Ce6 binding to LDL (5×10^{-8} M) following the fluorescence emission of Ce6 (excitation wavelength 408 nm). The curve was fitted by Eq. (11) with the following parameters: n_{Pi}: 10, K_{Pi}: 5×10^{6} M^{-1}, K_{L}: 7×10^{6} M^{-1}. The global binding constant, K_{LDL}, is 5.7×10^{7} M^{-1}.

curvature of the plot. The global affinity constant including all binding modes is 5.7×10^{7} M^{-1}.

3.3.3. Binding of Ce6 to LDL and pH effect

The overall affinity constant of chlorin for LDL can also be derived from Eq. (5) assuming that LDL possesses 10 binding sites. Fluorescence emission spectra of Ce6 (1×10^{-8} M) were recorded at different concentration of LDL. The overall concentration of binding sites on LDL was not in excess compared to the chlorin concentration in our experimental conditions. Hence, data were treated as described above for HSA to take free protein sites into account. The affinity of Ce6 for LDL is clearly pH dependent as shown in Fig. 5b. As high pH may affect the LDL integrity, we limited our investigation to pH 6.5 and 7.4. Results for LDL and HSA are compiled in Table 1. They clearly show an inverse dependence on pH of the affinities of HSA and LDL for Ce6.

4. Discussion

4.1. Solution properties of chlorin e6

These properties were examined in details by Cunderlikova et al. [7] as a function of pH. Upon pH decrease between 9 and 3.2, the chlorin fluorescence emission maximum was shifted from 661 to 648 nm. Depending on whether peak position or intensity of fluorescence was chosen by these authors to analyze data, the reported titration curves displayed inflection points at pH 5.9 or 6.5 [7]. Typical emission spectra in the pH range considered in the present study are reported in Fig. 3. In keeping with Cunderlikova's results a shoulder on the blue side of the emission band is observed at the lowest pH. Different processes may come into play to account for these changes. Firstly, the three carboxylic chains of chlorin e6 could be neutralized sequentially. For comparison, the pK_a values for a dicarboxylic porphyrin, deuteroporphyrin, were recently re-determined to be 6.6 and 5.3 [30]. In this compound, the fluorescence changes resulting from the neutralization of the carboxylate chains were interpreted more as a consequence of the favored formation of non-fluorescent dimers than as a direct modification of the spectroscopic properties of the macrocycle. This problem is not excluded with chlorin e6 even if it was more water-soluble owing to the presence of three carboxylic chains. It should be emphasized that these chains differ by the number of carbon atoms separating the carboxylic function from the macrocycle. A direct effect of the carboxylic group closely attached to the macrocycle on the spectroscopic properties might be supposed. However, as excited states of tetrapyrrolic compounds involve increased electronic distribution at the macrocycle periphery [31], the neutralization of the carboxylate would most likely lead to a spectral red shift. Alternatively, inner nitrogens can be protonated. In related carboxylic porphyrins, the pK_a value for the first inner nitrogen being protonated was found to be around 5.3 for deuteroporphyrin [30] and 5.0 for hematoporphyrin [32]. The blue shift of chlorin e6 emission might be due to protonation of the first inner nitrogen. It is conceivable that the pK of this nitrogen could be somewhat increased as compared to the value reported for porphyrins through the possibility of zwitterion formation with the carboxylate adjacent to the macrocycle. This does not exclude the neutralization of the other chains in the same pH range leading to a decrease of the overall charge and increase in lipophilicity. As a matter of fact, as reported by Cunderlikova et al. [7], the octanol–water partition coefficient of chlorin e6 increases with decreasing pH.

4.2. Chlorin e6 binding to membrane models

DOPC liposomes were chosen because of the low temperature of their main phase transition, − 18 °C [33], which permitted us to observe, at 20 °C, the interactions of Ce6 with the lipid bilayer in the liquid crystal phase. The red shift of the fluorescence excitation and emission maxima is indicative of incorporation of Ce6 into a hydrophobic environment [26]. In keeping with results obtained with related carboxylic porphyrins, it can be assumed that the chlorin macrocycle is buried into the hydrophobic lipid core and the carboxylic chains are oriented to the water interface [24,34]. The fluorescence characteristics of the chlorin bound to the liposomes were independent of pH indicating that in all cases, the free-base form, i.e. without inner nitrogen protonated, is incorporated into the bilayer. Similar behavior has been observed for porphyrins [35]. The binding constant of Ce6 to DOPC liposomes increases by about one order of magnitude when pH is lowered from 8.0 to 6.5. Obviously, this increase cannot involve the protonation of nitrogen, which would have the opposite effect. In this pH range, the phosphocholine head of DOPC is not subject to acid–base equilibria. Thus, only the neutralization of the carboxylic chains of the chlorin can account for the observed effect. The resulting increase of lipophilicity will result in an augmentation of its affinity for the membrane. In the case of Ce6, the relatively short lateral chains might restrict incorporation into the bilayer. In fact, preliminary experiments suggest that the transfer of this molecule through the bilayer is very slow (several hours). The affinity constant measured corresponds most likely to incorporation only into the outer hemileaflet of the vesicles. Accordingly, the affinity constant expressed as a function of accessible phospholipids should be divided by 0.558, the ratio between the lipids in the outer hemileaflet and the total number of lipids.

The value of the affinity constant of Ce6 to DOPC at pH 7.4 is significantly lower than that of deuteroporphyrin for egg phosphatidylcholine vesicles [36]. Both molecules possess a macrocycle of comparable lipophilicity, that of chlorin e6 with vinyl and ethyl chains being even larger. The difference in affinity appears to be related to the presence of three carboxylic groups instead of two for the porphyrin and to the shorter carboxylic chains in chlorin e6 impeding deep anchorage within the bilayer.

4.3. Chlorin e6 binding to human serum albumin

Albumin, the most abundant protein in human plasma, has a key role in the bioavailability and pharmacokinetics of drugs. Data on the binding of tetrapyrroles to albumin and their distribution among plasma proteins have been reviewed [19].

Most studies have focused on dicarboxylic porphyrins and heme, the iron complex of protoporphyrin. A high affinity binding site for porphyrin monomers has been identified [37,38]. In a series of dicarboxylic porphyrin from the less hydrophobic hematoporphyrin to the more hydrophobic protoporphyrin, the affinity constants have been found to range between about 1×10^6 and 3×10^8 M^{-1} [19]. No data on pH effect were available except for hematoporphyrin, the affinity of which is slightly higher in the pH range 6.8–7.5 (3.6×10^6 M^{-1}) than at pH 8 (1.27×10^6 M^{-1}) [39]. To our knowledge, there are very few reports [40] on the affinity of chlorins for albumin. At pH 7.4, chlorin e6 possesses an affinity constant of 1.8×10^8 M^{-1}, which is very similar to that of the more hydrophobic and less water-soluble deuteroporphyrin, 1.9×10^8 M^{-1} [41], and protoporphyrin, 2.8×10^8 M^{-1} [42]. In fact, chlorin e6 shares with these molecules a common assymetric structure. Their hydrophobic core bears polar carboxylic chains on one side only. It can be hypothesized that the high affinity site of dicarboxylic porphyrins or of chlorin e6 is identical to that of heme. This site has been characterized in subdomain IB of HSA. Heme is accommodated in a hydrophobic pocket with its propionate groups interacting with a triad of basic residues (lysine, arginine and histidine) at the pocket entrance [38]. Chlorin e6 could be accommodated in the same way, its three carboxylic groups providing even better stabilization via salt-bridges with the basic residues. The existence of at least four non-specific sites accommodating porphyrins with much lower affinity was also described [43], but these don't seem to influence the interactions in the concentration range studied. More likely, only low affinity sites were probed in Kochubeev's paper [40]. Interestingly, the affinity of chlorin e6 decreases when the pH is lowered from 8 to 6.5. This effect might be due to some neutralization of the carboxylic groups reducing salt-bridge stabilization. Besides, albumin was shown to undergo conformational changes in about the same pH range, which also could modify affinity for the chlorin [44].

4.4. Chlorin e6 binding to low density lipoproteins

The over-expression of LDL-receptors by neoplastic cells and the incorporation of photosensitizers associated to LDL have been suggested to contribute to the specific accumulation of photosensitizers in proliferative tissues [10–12]. This hypothesis has been supported by experiments on cells and tumor models. Among other examples, the cellular uptake and photoactivity of porphyrins are increased through potentialisation of LDL catabolism by lovastatin [45]. Preferential accumulation and retention of LDL-bound photosensitizers by a fibrosarcoma tumor in mouse has been reported [46]. By contrast, PDT resistant tumor cells have been shown to exhibit low activity of LDL related receptors [47]. Furthermore, experiments performed on an animal model with a very hydrophobic photosensitizer have revealed both a particularly high tumor uptake and an unprecedented high association with low-density lipoproteins [48]. However, the relevance of the low density lipoprotein receptor pathway for selective accumulation of the photosensitizer in tumors has been questioned [49,50]. The known tumor localizing ability of various photosensitizers is not correlated with their relative affinity for LDL [18] indicating that other mechanisms may come into play and/or other tumor compartments are also involved in selectivity. In addition, the LDL lipid structures might serve as a substrate for photoinduced peroxidation reactions and thus could enhance the overall biological efficiency of the photosensitizer [51]. Consequently, the affinity of photosensitizers for LDL and the number of molecules bound per LDL particle are important parameters. The distribution of the molecules between the different LDL compartments is important as well. This information has been derived from protein fluorescence quenching and from change in chlorin fluorescence upon binding to LDL.

In agreement with fluorescence quenching experiments, the results described above led to the identification of about ten sites close to the protein with a high intrinsic association constant ($K_{Pi}=5\times10^6$ M^{-1}), which corresponds to an overall affinity of 5×10^7 M^{-1}. In keeping with previous studies [27,29] and as derived in Results, non-specific binding to the lipid phase of LDL with a constant $K_L=7\times10^6$ M^{-1} also takes place. It may be noted that this constant is almost one order of magnitude lower than the overall affinity for the ten sites mentioned above. Taking into account the fact that one LDL particle contains about 800 molecules of phospholipids, the ratio $K_L/800$ leads to a lipid binding constant of 8.75×10^3 M^{-1}. It may be noted that this value is very close to that measured for DOPC liposomes after correction for accessible lipids (5.9×10^3 / 0.558 = 1×10^4 M^{-1}). Whatever the LDL/Ce6 ratio, the shape and position of the fluorescence emission spectra of the LDL-bound chlorin were the same, indicating that the environment of chlorin in the different LDL compartments is similar. Moreover, these spectra are like those observed during the incorporation of Ce6 into liposomes suggesting a hydrophobic environment in all cases. Comparable results were obtained with deuteroporphyrin [27]. This suggests that the first class of sites associated to tryptophan fluorescence quenching more likely involves the lipid–protein interface.

The global affinity constant at pH 7.4 calculated by the Scatchard's method, ($K_{LDL}=5.7\times10^7$ M^{-1}) or derived from Fig. 5 (6.9×10^7 M^{-1}) are in good agreement within experimental uncertainty. The global affinity constant of Ce6 for LDL is mainly governed by the fixation at "protein" sites and the partition into lipid compartments is rather a minority process. This affinity constant is about one order of magnitude lower than that determined for deuteroporphyrin [27]. As discussed above, the same difference was found in the case of binding to liposomes. This supports again the view that the "protein" sites more likely correspond to hydrophobic regions at the boundary between apoprotein B100 and the LDL lipid phase. The affinity of Ce6 for LDL is very close to that of aluminum phthalocyanine sulfonated on two adjacent isoindole units, AlPcS2a [52]. The decreased LDL affinity of AlPcS2a might be due to the permanent negative charge of the sulfonate groups, the pK of which is far below the physiological pH. In the case of Ce6 this might be due to the extra polar carboxylic group and/or

to the shortest lateral alkyl chains as compared to deuteroporphyrin. In keeping with the role of the charge of macrocycle side chains, we observed an increase of the global association constant by a factor of about 2 when the pH was decreased from 7.4 to 6.5. It may also be noted that each LDL particle binds about 10 Ce6 molecules, which is 5 times less than the value reported for more lipophilic photosensitizers [11,27].

4.5. The pH-dependent distribution of Chlorin e6 among plasma proteins

As outlined above, the relative distribution of photosensitizers between plasma components is an important determinant of their efficiency. Ultracentrifugation or gel exclusion chromatography experiments can give an overall picture of the distribution pattern. However, these two methods and/or differences in experimental protocols were found to yield conflicting results as reviewed by Kongshaug [19]. In the present work, we choose to derive quantitative binding data on isolated plasma proteins and membrane models. Albumin appears to be the major carrier in agreement with former data obtained by ultracentrifugation [21]. However, a striking feature of the data reported in Table 1 is the inverse dependence on pH of the affinity constants of Ce6 for HSA and LDL. The ratio K_{LDL}/K_{HSA} is multiplied by 4.6 when pH is decreased from 7.4 to 6.5. A parallel effect is expected for the partition of Ce6 between HSA and membranes, the ratio K_{DOPC}/K_{HSA} being multiplied by 3.5 for the same pH change. Although the concentrations of free chlorin or LDL-bound chlorin are expected to be fairly low, this pH effect might be significant.

Indeed, different studies have shown that the pH of the interstitial fluid in tumors is lower than that in the normal tissues [4,53,54]. This peculiarity reflects the excretion of lactic acid by tumor cells that present high rate of anaerobic glucose metabolism. The potential use of acid pH in tumors for therapeutic exploitation has been outlined [5,55], a suggestion also valid for carboxylic photosensitizers [56]. A comprehensive review of microelectrode measurements in human and animal tumors illustrating this effect has been published [53]. Although acidification is dependent on the size and histology of the tumor, the distributions of pH values obtained for subcutaneous normal tissues and tumors in human were found to have median values of about 7.5 and 7.0, respectively [53]. In a series of 14 human tumors of various histologies, Thistlethwaite [54] has reported a mean pH value of about 6.81. There was quite a large heterogeneity of pH within tumor and values as low as 5.55 were measured [54].

In the present study, we have selected a wide range of pH values in order to clearly illustrate, in vitro, the feasibility of a pH-dependent redistribution of chlorin e6 in the tumor stroma. We have quantified the change of chlorin e6 affinity towards HSA, LDL and lipid membranes as a function of pH. Although albumin is the major carrier for chlorin e6, some decrease of the stability of the Ce6–HSA complex and concomitant increase of binding to LDL and membranes upon small pH decrease could favor preferential uptake of such photosensitizers by tumors. These data illustrate the interest of quantitative information on the affinity of photosensitizers for their various carriers with emphasize on specific tumor properties, which could help in the rational design of more selective photosensitizers.

Acknowledgement

The authors thank James Grellier for his valuable comments on the manuscript.

References

[1] J.D. Spikes, Photodynamic reactions in photomedicine, in: J.D. Regan, J. A. Parrish (Eds.), The Science of Photomedicine, Plenum Press, New York, 1982, pp. 113–144.
[2] T.J. Dougherty, C.J. Gomer, B.W. Henderson, G. Jori, D. Kessel, M. Korbelik, J. Moan, Q. Peng, Photodynamic therapy, J. Natl. Cancer Inst. 90 (1998) 889–905.
[3] J. Moan, K. Berg, The photodegradation of porphyrins in cells can be used to estimate the lifetime of singlet oxygen, Photochem. Photobiol. 53 (1991) 549–553.
[4] P.M. Gullino, F.H. Grantham, S.H. Smith, A.C. Haggerty, Modifications of the acid–base status of the internal milieu of tumors, J. Natl. Cancer Inst. 34 (1965) 857–869.
[5] I.F. Tannock, D. Rotin, Acid pH in tumors and its potential for therapeutic exploitation, Cancer Res. 49 (1989) 4373–4384.
[6] J. Moan, L. Smedshammer, T. Christensen, Photodynamic effects on human cells exposed to light in the presence of hematoporphyrin. pH effects, Cancer Lett. 9 (1980) 327–332.
[7] B. Cunderlikova, L. Gangeskar, J. Moan, Acid–base properties of chlorin e6: relation to cellular uptake, J. Photochem. Photobiol., B Biol. 53 (1999) 81–90.
[8] J.P. Thomas, A.W. Girotti, Glucose administration augments in vivo uptake and phototoxicity of the tumor-localizing fraction of hematoporphyrin derivative, Photochem. Photobiol. 49 (1989) 241–247.
[9] K. Kuzelova, D. Brault, Interactions of dicarboxylic porphyrins with unilamellar lipidic vesicles: drastic effects of pH and cholesterol on kinetics, Biochemistry 34 (1995) 11245–11255.
[10] G. Jori, M. Beltramini, E. Reddi, B. Salvato, A. Pagnan, L. Ziron, L. Tomio, T. Tsanov, Evidence for a major role of plasma lipoproteins as hematoporphyrin carriers in vivo, Cancer Lett. 24 (1984) 291–297.
[11] J.P. Reyftmann, P. Morliere, S. Goldstein, R. Santus, L. Dubertret, D. Lagrange, Interaction of human serum low density lipoproteins with porphyrins: a spectroscopic and photochemical study, Photochem. Photobiol. 40 (1984) 721–729.
[12] D. Kessel, Porphyrin–lipoprotein association as a factor in porphyrin localization, Cancer Lett. 33 (1986) 183–188.
[13] P.C. de Smidt, T.J. van Berkel, LDL-mediated drug targeting, Crit. Rev. Ther. Drug Carr. Syst. 7 (1990) 99–120.
[14] Y.K. Ho, R.G. Smith, M.S. Brown, J.L. Goldstein, Low-density lipoprotein (LDL) receptor activity in human acute myelogenous leukemia cells, Blood 52 (1978) 1099–1114.
[15] D. Gal, M. Ohashi, P.C. MacDonald, H.J. Buchsbaum, E.R. Simpson, Low-density lipoprotein as a potential vehicle for chemotherapeutic agents and radionucleotides in the management of gynecologic neoplasms, Am. J. Obstet. Gynecol. 139 (1981) 877–885.
[16] J.P. Segrest, M.K. Jones, H. De Loof, N. Dashti, Structure of apolipoprotein B-100 in low density lipoproteins, J. Lipid Res. 42 (2001) 1346–1367.
[17] R.M. Bohmer, G. Morstyn, Uptake of hematoporphyrin derivative by normal and malignant cells: effect of serum, pH, temperature, and cell size, Cancer Res. 45 (1985) 5328–5334.
[18] M. Kongshaug, J. Moan, S.B. Brown, The distribution of porphyrins with different tumour localising ability among human plasma proteins, Br. J. Cancer 59 (1989) 184–188.
[19] M. Kongshaug, Distribution of tetrapyrrole photosensitizers among human plasma proteins, Int. J. Biochem. 24 (1992) 1239–1265.

[20] D. Kessel, K.L. Whitcomb, V. Schulz, Lipoprotein-mediated distribution of N-aspartyl chlorin-E6 in the mouse, Photochem. Photobiol. 56 (1992) 51–56.
[21] B. Cunderlikova, M. Kongshaug, L. Gangeskar, J. Moan, Increased binding of chlorin e(6) to lipoproteins at low pH values, Int. J. Biochem. Cell. Biol. 32 (2000) 759–768.
[22] F. Yuan, M. Dellian, D. Fukumura, M. Leunig, D.A. Berk, V.P. Torchilin, R.K. Jain, Vascular permeability in a human tumor xenograft: molecular size dependence and cutoff size, Cancer Res. 55 (1995) 3752–3756.
[23] A. Orenstein, G. Kostenich, L. Roitman, Y. Shechtman, Y. Kopolovic, B. Ehrenberg, Z. Malik, A comparative study of tissue distribution and photodynamic therapy selectivity of chlorin e6, Photofrin II and ALA-induced protoporphyrin IX in a colon carcinoma model, Br. J. Cancer 73 (1996) 937–944.
[24] K. Kuzelova, D. Brault, Kinetic and equilibrium studies of porphyrin interactions with unilamellar lipidic vesicles, Biochemistry 33 (1994) 9447–9459.
[25] A. Sytnik, I. Litvinyuk, Energy transfer to a proton-transfer fluorescence probe: tryptophan to a flavonol in human serum albumin, Proc. Natl. Acad. Sci. U. S. A. 93 (1996) 12959–12963.
[26] K. Das, B. Jain, A. Dube, P.K. Gupta, pH dependent binding of chlorin p-6 with phosphatidyl choline liposomes, Chem. Phys. Lett. 401 (2005) 185–188.
[27] S. Bonneau, C. Vever-Bizet, P. Morliere, J.C. Maziere, D. Brault, Equilibrium and kinetic studies of the interactions of a porphyrin with low-density lipoproteins, Biophys. J. 83 (2002) 3470–3481.
[28] C.R. Cantor, P.R. Schimmel, Biophysical Chemistry, Part II: Techniques for the Study of Biological Structure and Function, W. H. Freeman, San Francisco, 1980.
[29] M. Beltramini, P.A. Firey, F. Ricchelli, M.A. Rodgers, G. Jori, Steady-state and time-resolved spectroscopic studies on the hematoporphyrin–lipoprotein complex, Biochemistry 26 (1987) 6852–6858.
[30] S. Bonneau, N. Maman, D. Brault, Dynamics of pH-dependent self-association and membrane binding of a dicarboxylic porphyrin: a study with small unilamellar vesicles, Biochim. Biophys. Acta 1661 (2004) 87–96.
[31] C. Weiss, Electronic absorption spectra of chlorophylls, in: D. Dolphin (Ed.), The Porphyrins, Academic Press, New York, 1978, pp. 211–223.
[32] D. Brault, C. Vever-Bizet, Protonation equilibria of haematoporphyrin as studied by fluorescence lifetime analysis, J. Chem. Soc., Faraday Trans. 88 (1992) 1519–1524.
[33] G. Cevc, Phospholipids Handbook, Marcel Dekker, New York, 1993.
[34] I. Bronshtein, M. Afri, H. Weitman, A.A. Frimer, K.M. Smith, B. Ehrenberg, Porphyrin depth in lipid bilayers as determined by iodide and parallax fluorescence quenching methods and its effect on photosensitizing efficiency, Biophys. J. 87 (2004) 1155–1164.
[35] D. Brault, C. Vever-Bizet, K. Kuzelova, Interactions of dicarboxylic porphyrins with membranes in relation to their ionization state, J. Photochem. Photobiol., B Biol. 20 (1993) 191–195.
[36] D. Brault, C. Vever-Bizet, T. Le Doan, Spectrofluorimetric study of porphyrin incorporation into membrane models — Evidence for pH effects, Biochim. Biophys. Acta 857 (1986) 238–250.
[37] M. Wardell, Z. Wang, J.X. Ho, J. Robert, F. Ruker, J. Ruble, D.C. Carter, The atomic structure of human methemalbumin at 1.9 A, Biochem. Biophys. Res. Commun. 291 (2002) 813–819.
[38] P.A. Zunszain, J. Ghuman, T. Komatsu, E. Tsuchida, S. Curry, Crystal structural analysis of human serum albumin complexed with hemin and fatty acid, BMC Struct. Biol. 3 (2003) 6.
[39] E. Reddi, F. Ricchelli, G. Jori, Interaction of human serum albumin with hematoporphyrin and its Zn(2)+- and Fe(3)+-derivatives, Int. J. Pept. Protein Res. 18 (1981) 402–408.
[40] G.A. Kochubeev, A.A. Frolov, E.I. Zen'kevich, G.P. Gurinovich, Characteristics of complex-formation of chlorine e6 with human and bovine serum albumins, Mol. Biol. (Mosk.) 22 (1988) 968–975.
[41] G.A. Moehring, A.H. Chu, L. Kurlansik, T.J. Williams, Heterogeneity of albumin as detected by its interactions with deuteroporphyrin IX, Biochemistry 22 (1983) 3381–3386.
[42] M. Rotenberg, S. Cohen, R. Margalit, Thermodynamics of porphyrin binding to serum albumin: effects of temperature, of porphyrin species and of albumin-carried fatty acids, Photochem. Photobiol. 46 (1987) 689–693.
[43] G.H. Beaven, S.H. Chen, A. d' Albis, W.B. Gratzer, A spectroscopic study of the haemin–human–serum–albumin system, Eur. J. Biochem. 41 (1974) 539–546.
[44] W.J. Leonard Jr., K.K. Vijai, J.F. Foster, A structural transformation in bovine and human plasma albumins in alkaline solution as revealed by rotatory dispersion studies, J. Biol. Chem. 238 (1963) 1984–1988.
[45] S. Biade, J.C. Maziere, L. Mora, R. Santus, C. Maziere, M. Auclair, P. Morliere, L. Dubertret, Lovastatin potentiates the photocytotoxic effect of photofrin II delivered to HT29 human colonic adenocarcinoma cells by low density lipoprotein, Photochem. Photobiol. 57 (1993) 371–375.
[46] A. Barel, G. Jori, A. Perin, P. Romandini, A. Pagnan, S. Biffanti, Role of high-, low- and very low-density lipoproteins in the transport and tumor-delivery of hematoporphyrin in vivo, Cancer Lett. 32 (1986) 145–150.
[47] M.C. Luna, A. Ferrario, N. Rucker, C.J. Gomer, Decreased expression and function of alpha-2 macroglobulin receptor/low density lipoprotein receptor-related protein in photodynamic therapy- resistant mouse tumor cells, Cancer Res. 55 (1995) 1820–1823.
[48] M. Soncin, L. Polo, E. Reddi, G. Jori, B.D. Rihter, M.E. Kenney, M.A. Rodgers, Unusually high affinity of Zn(II)-tetradibenzobarrelenooctabutoxy- phthalocyanine for low-density lipoproteins in a tumor-bearing mouse, Photochem. Photobiol. 61 (1995) 310–312.
[49] M. Korbelik, J. Hung, Cellular delivery and retention of Photofrin II: the effects of interaction with human plasma proteins, Photochem. Photobiol. 53 (1991) 501–510.
[50] M. Korbelik, Low density lipoprotein receptor pathway in the delivery of Photofrin: how much is it relevant for selective accumulation of the photosensitizer in tumors? J. Photochem. Photobiol., B Biol. 12 (1992) 107–109.
[51] J. Martins, V. Madeira, L. Almeida, J. Laranjinha, Photoactivation of phthalocyanine-loaded low density lipoproteins induces a local oxidative stress that propagates to human erythrocytes: protection by caffeic acid, Free Radic. Res. 36 (2002) 319–328.
[52] S. Bonneau, P. Morliere, D. Brault, Dynamics of interactions of photosensitizers with lipoproteins and membrane-models: correlation with cellular incorporation and subcellular distribution, Biochem. Pharmacol. 68 (2004) 1443–1452.
[53] J.L. Wike-Hooley, J. Haveman, H.S. Reinhold, The relevance of tumour pH to the treatment of malignant disease, Radiother. Oncol. 2 (1984) 343–366.
[54] A.J. Thistlethwaite, D.B. Leeper, D.J. Moylan III, R.E. Nerlinger, pH distribution in human tumors, Int. J. Radiat. Oncol. Biol. Phys. 11 (1985) 1647–1652.
[55] L.E. Gerweck, K. Seetharaman, Cellular pH gradient in tumor versus normal tissue: potential exploitation for the treatment of cancer, Cancer Res. 56 (1996) 1194–1198.
[56] R. Pottier, J.C. Kennedy, New Trends in Photobiology (Invited Review) The possible role of ionic species in selective biodistribution of photochemotherapeutic agents toward neoplastic tissue, J. Photochem. Photobiol., B Biol. 8 (1990) 1–16.